

Atom Transfer Radical Polymerization of Methyl Methacrylate Mediated by Grubbs 1st and 2nd Generation Catalysts: Insight into the Active Species

Maria Beatriz A. Afonso,^a Lucas G. Gonçalves,^a Patrícia Borim,^a José Luiz S. Sá,^b Beatriz E. Goi^a and Valdemiro P. Carvalho-Jr.*^a

^aFaculdade de Ciências e Tecnologia, Universidade Estadual Paulista, 19060-900 Presidente Prudente-SP, Brazil

^bDepartamento de Química, GERATEC, Universidade Estadual do Piauí, 64002-150 Teresina-PI, Brazil

Ruthenium benzylidene complexes were evaluated as catalysts in atom-transfer radical polymerization (ATRP) of methyl methacrylate (MMA) under different reaction conditions. The mechanism by which Grubbs 1st and 2nd generation catalysts mediate olefin metathesis has been studied, little is known regarding the mechanism of ATRP reaction promoted by these complexes. Conversion and semilogarithmic kinetic plots as a function of time were correlated to the different catalysts and reaction conditions; especially in the presence of Al(O*i*Pr)₃ as additive. Molecular weight (*M_n*) and polydispersity index (PDI) values changed with different catalysts in the presence or absence of Al(O*i*Pr)₃. Kinetic studies by ¹H NMR revealed that two complexes in the presence of Al(O*i*Pr)₃ are converted into ATRP-active with the dissociation of PCy₃, but with the benzylidene group preserved. More controlled polymerizations were achieved using Grubbs 1st and, the presence of Al(O*i*Pr)₃ improved the control levels for both catalysts.

Keywords: methyl methacrylate, ruthenium, ATRP, Grubbs catalysts

Introduction

Atom-transfer radical polymerization (ATRP) is a catalyst-based process which the growing radicals can be reversibly activated or deactivated via a dynamic equilibrium with a transition metal complex with an exchange of halogen atom between the chain and metal complex.¹⁻¹³ A variety of metal complexes used as catalysts in the reaction provides the control of the molecular weight distribution, which in turn can enable the facile synthesis of well-defined polymers.¹⁴⁻¹⁷

Ruthenium-based metathesis catalysts have shown an excellent application profile in obtaining such polymers using the ATRP protocol.¹⁸⁻²¹ This area of research has attracted widespread interest, since the first report of ruthenium-based catalysts, although this system itself was not effective in methyl methacrylate (MMA) polymerization, but the addition of an aluminum alkoxides such as Al(O*i*Pr)₃ accelerated the reaction and produced polymers with narrow with narrow

molecular weight distributions (PDIs).² The efficiency and versatility of Grubbs 1st (**1**) and 2nd (**2**) generation metathesis catalysts for promoting ATRP of vinyl monomers was already reported.^{22,23} The ability of these catalysts to promote two reactions with such markedly different mechanisms has been utilized in various tandem reactions in which olefin metathesis and atom transfer radical reactions take place in one pot.²⁴ As complexes **1** and **2** were known to be highly active for ring-opening metathesis polymerization (ROMP) and ATRP reactions, however, while the mechanism of olefin metathesis with these catalysts has been well-studied, the mechanism by which ruthenium benzylidenes promote ATRP reactions remains unknown. Thus, their dual behavior prompted us to explore the yet unknown mechanism for ATRP mediated by these catalysts (Figure 1).

The present study is aimed to optimize the reaction conditions for the controlled polymerization of MMA by ATRP using **1** or **2**. Thus, the homopolymerization of MMA via ATRP using **1** or **2** in different reaction conditions were investigated. The complexes **1** and **2** were able to mediate these polymerizations with acceptable rate and level of control.

*e-mail: valdemiro@fct.unesp.br

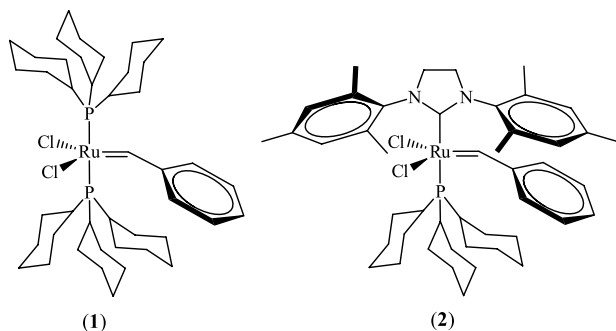


Figure 1. Structures of Grubbs 1st (1) and 2nd (2) generation catalysts.

Experimental

General details

All reagents were purchased from Aldrich Chemical Co. All reactions and manipulations were conducted under a nitrogen atmosphere using standard Schlenk techniques. Toluene was dried overnight over calcium chloride, filtered and distilled from sodium benzophenone ketyl and degassed by three vacuum-nitrogen cycles under nitrogen before use. The monomers methyl methacrylate (MMA) and ethyl methacrylate (EMA) were washed with 5% NaOH solution, dried over anhydrous MgSO₄, vacuum distilled from CaH₂ and stored at -18 °C before use. Grubbs 1st and 2nd generation catalysts, anisole, 2,2,6,6-tetramethyl-1-piperidinyloxy (TEMPO), tetrabutylammonium hexafluorophosphate (*n*-Bu₄NPF₆), aluminium isopropoxide (Al(O*i*Pr)₃) and ethyl 2-bromoisobutyrate (EB*i*B) were used as acquired.

ATRP procedure

A ruthenium complex (23.5 μmol) was placed in a Schlenk tube containing a magnet bar and capped with a rubber septum. Air was expelled by three vacuum-nitrogen cycles before the monomer (MMA; 4.71 mmol) and the initiator solution (EB*i*B; 48.2 μmol) were added. All liquids were handled with dried syringes under nitrogen. The tube was capped under N₂ atmosphere using Schlenk techniques, then the reaction mixture was magnetically stirred and heated in a thermostated oil bath at 85 °C. Aliquots (20 μL) were removed at appropriate intervals.

Analyses

Conversion was determined from the concentration of residual monomer measured by gas chromatography (GC) using a Shimadzu GC-2010 gas chromatograph equipped with flame ionization detector and a 30 m (0.53 mm i.d., 0.5 μm film thickness) SPB-1 Supelco

fused silica capillary column. Anisole was added to polymerization and used as an internal standard. Analysis conditions: injector and detector temperature, 250 °C; temperature program, 40 °C (4 min), 20 °C min⁻¹ until 200 °C, 200 °C (2 min). The molecular weights and the molecular weight distribution of the polymers were determined by gel permeation chromatography using a Shimadzu Prominence LC system equipped with a LC-20AD pump, a DGU-20A5 degasser, a CBM-20A communication module, a CTO-20A oven at 40 °C, and a RID-10A detector equipped with two Shimadzu columns (GPC-805: 30 cm, Ø = 8.0 mm). The retention time was calibrated with standard monodispersed polyMMA using HPLC-grade THF as an eluent at 40 °C with a flow rate of 1.0 mL min⁻¹. Theoretical molecular weights (*M*_{n,th}) were calculated without considering the end groups according to the following equation: $M_{n,th} = ([\text{Monomer}]_0 / [\text{Initiator}]_0) \times \text{Conversion} \times \text{Monomer molecular weight}$. Electrochemical measurements were performed using an Autolab PGSTAT 204 potentiostat with a stationary platinum disk and a wire as working and auxiliary electrodes, respectively. The reference electrode was Ag/AgCl. The measurements were performed at 25 ± 0.1 °C in CH₂Cl₂ with 0.1 mol L⁻¹ of *n*-Bu₄NPF₆. The *E*_{1/2} values were the arithmetic average of the anodic and cathodic potential peaks (*E*_{p,a} + *E*_{p,c})/2. UV-Vis measurements were performed on a Cary 400 UV-Vis spectrophotometer (Varian) using 1 cm path length quartz cells. Toluene solutions of the complexes of 0.1 mM concentrations were used for these measurements. The ¹H and ³¹P{¹H} nuclear magnetic resonance (NMR) spectra were obtained in CDCl₃ at 298 K on a Bruker DRX-400 spectrometer operating at 400.13 and 161.98 MHz, respectively. The obtained chemical shifts were reported in ppm relative to TMS or 85% H₃PO₄.

Results and Discussion

The polymerizations were performed in the presence or in the absence of Al(O*i*Pr)₃ with an initial molar ratio of [Monomer]/[EB*i*B]/[Ru] = 200/2/1. With **1** as catalyst in the absence of Al(O*i*Pr)₃ at 85 °C, the MMA polymerization took 4 h to reach 10% conversion, and considerably increased to 90% after 16 h of reaction, whereas with **2** under similar conditions, only 5% of conversion was reached after 4 h, increasing to 25% in 16 h of reaction. With Al(O*i*Pr)₃, the conversion values for both catalysts were similar, increasing from 30 to 60% as the reaction time increased from 4 to 16 h (Figure 2). The plot of ln ([M]₀/[M]) as a function of the reaction time shows an asymptotic relationship for both catalysts, revealing that the radical concentration is not constant during the MMA polymerization (Figure 2, insert).

Table 1. ATRP^a of MMA in the presence or absence of Al(O*i*Pr)₃ using **1** or **2** in toluene

	Condition	Conversion ^b / %	$M_n^c \times 10^3$	PDI	f^d
1	without Al	95 ^f	66.0	1.28	0.6
		90	6.0	1.32	1.5
	with Al ^e	63	9.1	1.32	0.7
2	without Al	25	3.5	1.92	0.6
	with Al ^e	59	13.8	1.86	0.4

^a[monomer]/[initiator]/[Ru] = 200/2/1 molar ratio, T = 85 °C, reaction time = 16 h; ^bdetermined from the concentration of residual monomer measured by gas chromatography (GC); ^cdetermined with size exclusion chromatography (SEC) with polystyrene calibration; ^dinitiation efficiency $f = M_{n,theor}/M_{n,exp}$ with $M_{n,theor} = ([monomer]/[initiator]) \times M_{w,(monomer)} \times conversion$; ^e[Al(O*i*Pr)₃]/[Ru] = 4 molar ratio; ^f[monomer]/[initiator]/[Ru] = 800/2/1 molar ratio, T = 85 °C, reaction time = 16 h.²²

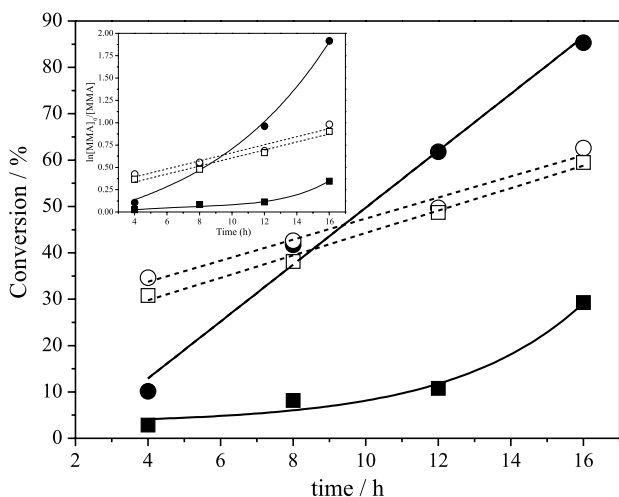


Figure 2. Dependence of conversion on the reaction time for ATRP of MMA in the presence and absence of Al(O*i*Pr)₃ using **1** or **2** in toluene at 85 °C. (●) [MMA]/[EBiB]/[1]/[Al] = 200/2/1/0; (■) [MMA]/[EBiB]/[2]/[Al] = 200/2/1/0; (○) [MMA]/[EBiB]/[1]/[Al] = 200/2/1/4; (□) [MMA]/[EBiB]/[2]/[Al] = 200/2/1/4. Insert: semilogarithmic plots on the reaction time for ATRP of MMA in the presence or absence of Al(O*i*Pr)₃ using **1** or **2**.

Similar result was observed in ATRP mediated by a Ru compound and CCl₄ as initiator; this fact was interpreted as an indicative that the propagating species were consumed only in the termination reactions. In addition, the literature highlights that, in similar cases, no M_n dependence on conversion could be observed.²⁵ However, the M_n values obtained in the reaction grew with conversion accompanied by decreasing PDI values when using both catalysts (Figure 3). When analyzing the control on the polymerization of MMA when using **1** or **2**, the ratio between the experimental and theoretical molecular weight values shows that the molecular weights of polyMMA were far below or above than the predicted one. The narrowest molecular weight distribution was obtained with **1** for [MMA]/[Ru] = 800, although the M_n was higher than the calculated value (initiation efficiency factor (f) = 0.6).²² With [MMA]/[Ru] = 200, the initiation efficiency factor

was then higher than 1 ($f = 1.5$), indicating the generation of additional polymer chains through transfer reactions (Table 1). Broader PDI values resulted from substitution of one PCy₃ in **1** by a *N*-heterocyclic carbene in **2**.

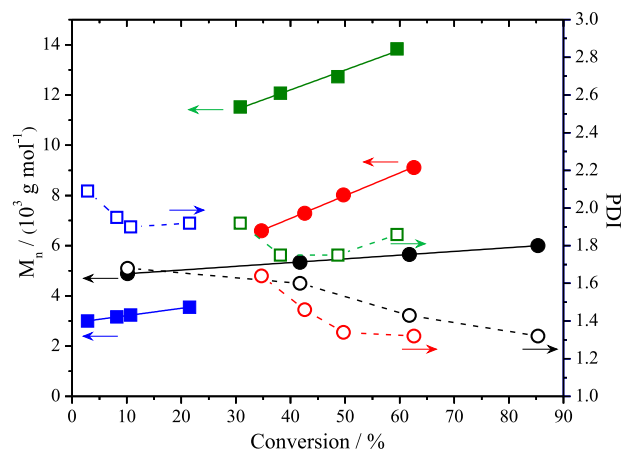


Figure 3. Dependence of M_n (solid) and PDI (hollow) values on conversion for ATRP of MMA in the presence or absence of Al(O*i*Pr)₃ using **1** or **2** in toluene at 85 °C. [MMA]/[EBiB]/[Ru] = 200/2/1; (●, ○) [1]/[Al] = 1/0; (■, □) [2]/[Al] = 1/0; (●, ○) [1]/[Al] = 1/4; (■, □) [2]/[Al] = 1/4.

Polymerizations were also carried out with **1** and **2** under similar conditions in the presence of Al(O*i*Pr)₃. For both catalysts, the linear dependence of $\ln([M]_0/[M])$ on time, with $k_{obs} = 1.25 \times 10^{-5} \text{ s}^{-1}$ for **1** and $k_{obs} = 1.24 \times 10^{-5} \text{ s}^{-1}$ for **2**, and the linear increase of molecular weight with conversion coupled with lower PDIs (Figures 2 and 3), illustrate an improvement of the control that **1** or **2** exert over MMA polymerization. However, the improvement was more pronounced for **1**, which M_n values are in good agreement with those theoretically calculated, with initiation efficiency factor nearer of 1 ($f = 0.7$) when compared that performed in the absence of Al(O*i*Pr)₃ (Table 1).

Recently, the importance of the characteristics of complexes in relation to the nature of ligands in the coordination sphere has been highlighted in the radical polymerization of methacrylates when proceeding in

the presence of $\text{Al}(\text{O}i\text{Pr})_3$.²⁶⁻²⁸ As previously seen, the presence of $\text{Al}(\text{O}i\text{Pr})_3$ plays an important role in the control of polymerizations; therefore, we proceed the UV-Vis spectroscopy study to observe what occurs in the reaction mixture (Figure 4). UV-Vis spectra were registered in the interval of 20 min for 3 h with **1** or **2** in presence or in the absence of $\text{Al}(\text{O}i\text{Pr})_3$. No variation was observed when comparing the spectra in presence or in the absence of $\text{Al}(\text{O}i\text{Pr})_3$ for up to 3 h. It was interpreted that there was no coordination of the additive to the complex, because other bands were not observed, at least in the metal with oxidation state +2. The stability of **1** and **2** in solution was also evaluated as a function of time at 50 °C by NMR (Figures S1 and S2). In both complexes, the appearance of the sign at 48.9 ppm shows that a PCy_3 leaves the ruthenium center, which the PCy_3 dissociation from **1** is faster than **2**. Thus, the decrease in the absorption observed in the electronic spectra of the catalysts in the presence or absence of Al additive can be related to the release of PCy_3 from the

coordination sphere of the benzylidene complexes.

Since ATRP depends on a single electron redox couple, electrochemical techniques provide useful insight into which complexes should be suitable catalysts for ATRP.²⁻¹² The cyclic voltammogram of **1** and **2** (Figure 5) presented a redox process in the potential range from 0.2 to 0.9 V, corresponding to the $\text{Ru}^{\text{II}}/\text{Ru}^{\text{III}}$ conversion with $E_{1/2} = 0.66$ V for **1** and $E_{1/2} = 0.55$ V for **2** vs. Ag/AgCl . The cyclic voltammetry of **1** showed the anodic process corresponding to the $\text{Ru}^{\text{II}}/\text{Ru}^{\text{III}}$ conversion at $E_{\text{pa}} = 0.74$ V, and a small cathodic process was detected at $E_{\text{pc}} = 0.59$ V. Although the $\text{Ru}^{\text{II}}/\text{Ru}^{\text{III}}$ redox cycle of **1** seems chemically irreversible during the electrochemical redox process, the absence of a complete reduction indicates that the Ru^{III} species is not stable, and immediately decomposes into other species that cannot regenerate the Ru^{II} species. In contrast, the cyclic voltammogram of **2** shows a quasi-reversible redox couple where the anodic and cathodic process were clearly observed at $E_{\text{pa}} = 0.69$ V and $E_{\text{pc}} = 0.40$ V, respectively.

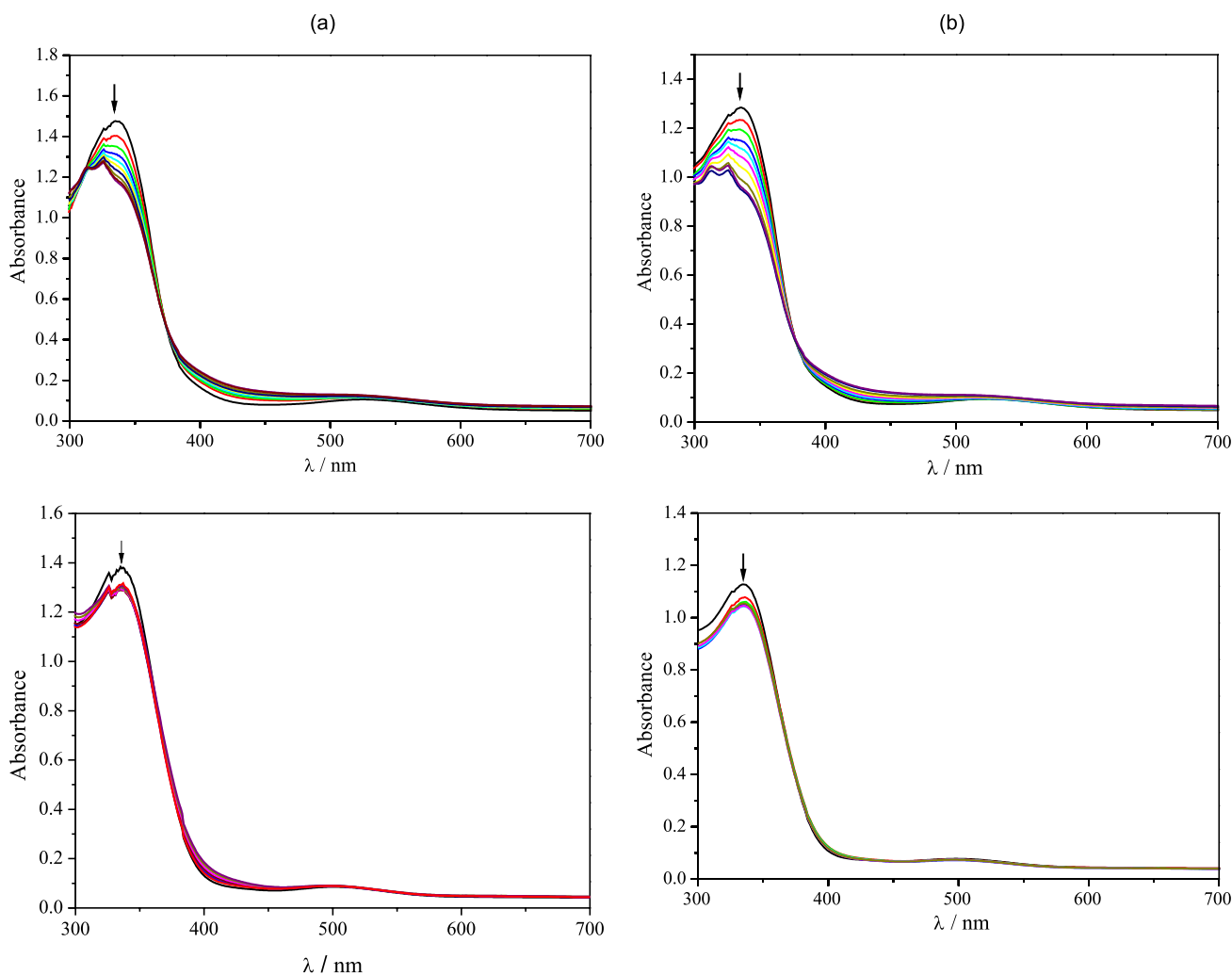


Figure 4. Absorption spectra of **1** (above) and **2** (below) in the (a) absence and (b) presence of $\text{Al}(\text{O}i\text{Pr})_3$ in toluene; $[\text{Ru}] = 0.1 \text{ mmol L}^{-1}$; $[\text{Al}]/[\text{1}] = 4$.

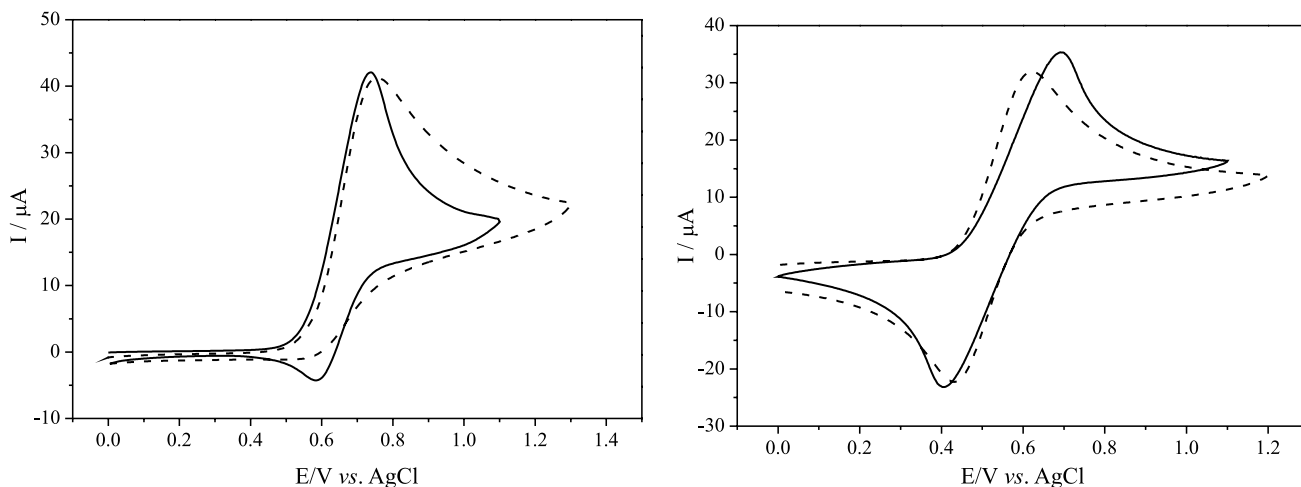


Figure 5. Cyclic voltammogram of **1** (left) and **2** (right) in the absence (solid line) and presence (dash line) of $\text{Al}(\text{O}i\text{Pr})_3$ in CH_2Cl_2 , at 25 °C. $[\text{Ru}] = 10 \text{ mM}$; $[\textit{n}\text{-Bu}_4\text{NPF}_6] = 100 \text{ mM}$ (supporting electrolyte). Scan rate = 100 mV s^{-1} .

The cyclic voltammogram data confirm the greater reducing power of **2** containing a more electron-donating ligand. However, the correlation does not directly extend to the quality of an ATRP catalyst. The reversibility of the redox couple is also important. For example in the case of **2** the redox potential is lower than that for **1**, but the peak-to-peak separation is almost twice larger ($\Delta E_p = 150 \text{ mV}$ for **1** and $\Delta E_p = 290 \text{ mV}$ for **2**) and, as consequence, **2** undergoes a more sluggish electron transfer, possibly as a result of a more substantial reorganization of the Ru center during the electron-transfer process.

Studies show that the polymerization of vinyl monomer via ATRP mediated by Ru catalysts in the presence of metal alkoxides, for instance $\text{Al}(\text{O}i\text{Pr})_3$, in some cases, increases the polymerization rate and affords polymers of controlled molecular weights by interaction with the ruthenium complex and thereby stabilizes the higher oxidation state Ru^{III} species to facilitate radical generation from a dormant species.²⁹ The electrochemical

properties of **1** and **2** in the presence of $\text{Al}(\text{O}i\text{Pr})_3$ were also investigated by cyclic voltammetry to investigate possible interactions between complex (**1** or **2**) and the Al additive (Figure 5). However, changes in redox processes and the appearance of new processes were not observed in both cases, corroborating the UV-Vis studies. Moreover, the presence of $\text{Al}(\text{O}i\text{Pr})_3$ did not provide an increase in the electrochemical reversibility of **1** and **2**. The $^{31}\text{P}\{^1\text{H}\}$ NMR spectrum of **1** obtained from the experiment in the presence of EB*i*B, $\text{Al}(\text{O}i\text{Pr})_3$ and MMA at 50 °C showed the decrease of the initial peak at 35.3 ppm while a new peak arose at 35.8 ppm assigned to bromide complex $[\text{RuCl}_2\text{Br}(\text{=CHPh})(\text{PCy}_3)]$, with the appearance of the signal at 48.9 ppm attributed to the free PCy_3 produced in the solution after dissociation from **1** (Figure 6, right). This is a clear indication that the PCy_3 leaves the complex to produce a five-coordinated bromide-Ru species via a dissociative type mechanism. Similar results were observed with **2** (Figure 6, left).

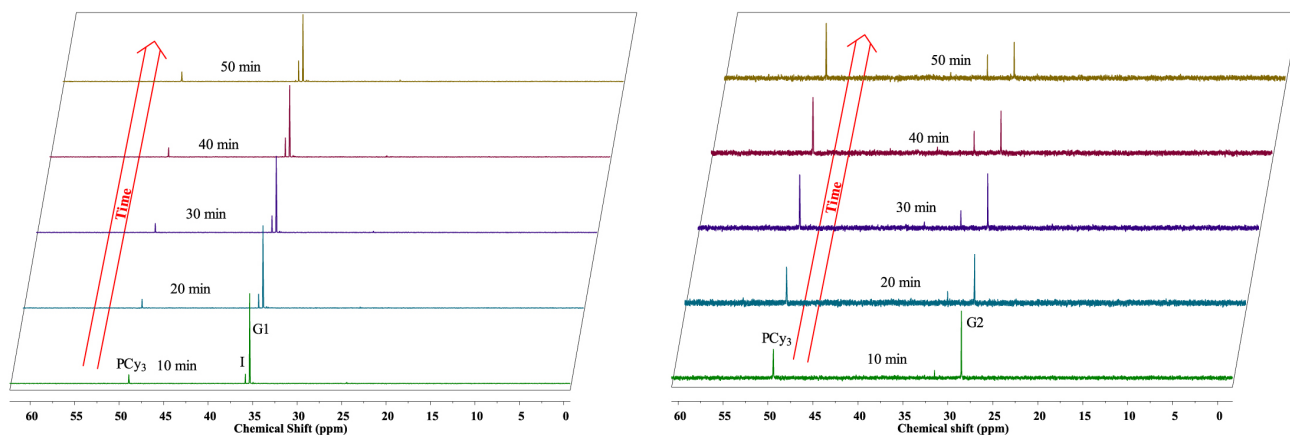
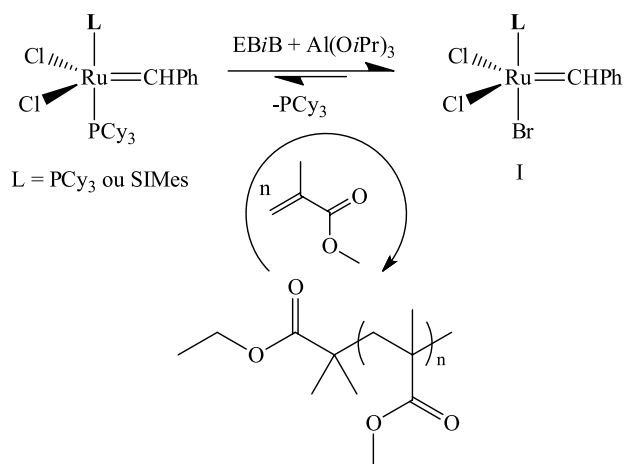


Figure 6. $^{31}\text{P}\{^1\text{H}\}$ -NMR spectra of **1** (left) and **2** (right) in the presence of EB*i*B, $\text{Al}(\text{O}i\text{Pr})_3$ and MMA as a function of time in CDCl_3 at 50 °C; $[\text{MMA}]/[\text{EB}i\text{B}]/[\text{Al}] = 200/2/4/1$.

In order to investigate whether ATRP is mediated by ruthenium species without decomposition of the benzylidene moiety, the signal of carbene metal was monitored during polymerization by ^1H NMR (Figure S3). In fact, there is a consumption signal assigned to the benzylidene group from the initial species, but the appearance of a new signal was also observed, confirming that the metal carbene is preserved in the active species during ATRP of MMA under these conditions. Thus, the ATRP of MMA mediated by **1** or **2** in the presence of $\text{Al}(\text{O}i\text{Pr})_3$ will occur when the PCy_3 molecule undergoes discoordination from the metal center (Scheme 1). We believe that the Al additive plays an important factor in ATRP mechanism mediated by **1** or **2**, preserving the benzylidene group in the active species, different from the polymerization performed in the absence of additive, wherein the benzylidene group is decomposed.^{22,23} Although a detailed study has been conducted to try to elucidate the action of Al additive in the ATRP reaction, the origins of these effects are still under investigation.



Scheme 1. Possible reaction routes for ATRP of MMA mediated by **1** or **2** in the presence of $\text{Al}(\text{O}i\text{Pr})_3$.

The cyclic voltammetry, UV-Vis and NMR studies help us build an understanding about the differences in the reactivity of the catalysts **1** and **2** in the polymerization of MMA. Initially, it should be emphasized that the redox properties of **1** or **2** for ATRP are important, but not decisive for their efficiency, as proof, electrochemical profiles confirm a greater reversibility to the precursor **2**, however, the best results came from **1**. On the other hand, kinetic studies show the output of PCy_3 from **1** is faster than **2**, accessing the active species efficiently.

Conclusion

The catalysts **1** or **2** were successfully applied for ATRP

of MMA in the presence or in the absence of $\text{Al}(\text{O}i\text{Pr})_3$. Both catalysts showed reasonable control of MMA polymerization in the absence of $\text{Al}(\text{O}i\text{Pr})_3$ but the control in ATRP is improved in the presence of Al additive. The ^1H and ^{31}P NMR studies of **1** or **2** obtained from the experiment in the presence of EBiB , $\text{Al}(\text{O}i\text{Pr})_3$ and MMA showed that the PCy_3 leaves the initial complex to produce a five-coordinated bromide-Ru species without decomposition of the benzylidene moiety via a dissociative type mechanism. Kinetic studies show the output of PCy_3 from **1** is faster than **2**, accessing the active species efficiently and that Al additive plays as an important tool during the catalysis.

Supplementary Information

Supplementary data are available free of charge at <http://jbcs.sbq.org.br> as PDF file.

Acknowledgments

The authors are indebted to the financial support from FAPESP (Proc. 2013/10002-0) and Prope (Proc. 2180/002/14-PROPe/CDC). The 400 MHz NMR analyses were performed at the Instituto de Química de São Carlos, IQSC/USP, São Carlos, SP, Brazil.

References

- Braunecker, W. A.; Matyjaszewski, K.; *Prog. Polym. Sci.* **2007**, *32*, 93.
- Kato, M.; Kamigaito, M.; Sawamoto, M.; Higashimura, T.; *Macromolecules* **1995**, *28*, 1721.
- Wang, J. S.; Matyjaszewski, K.; *J. Am. Chem. Soc.* **1995**, *117*, 5614.
- Matyjaszewski, K.; Tsarevsky, N. V.; *Nat. Chem.* **2009**, *4*, 276.
- Di Lena, F.; Matyjaszewski, K.; *Prog. Polym. Sci.* **2010**, *35*, 959.
- Lee, H.; Pietrasik, J.; Sheiko, S. S.; Matyjaszewski, K.; *Prog. Polym. Sci.* **2010**, *35*, 24.
- Sieglwart, D. J.; Oh, J. K.; Matyjaszewski, K.; *Prog. Polym. Sci.* **2012**, *37*, 18.
- Matyjaszewski, K.; *Macromolecules* **2012**, *45*, 4015.
- Wever, D. A. Z.; Raffa, P.; Picchioni, F.; Broekhuis, A. A.; *Macromolecules* **2012**, *45*, 4040.
- Matyjaszewski, K.; Tsarevsky, N. V.; *J. Am. Chem. Soc.* **2014**, *136*, 6513.
- Chmielarz, P.; Park, S.; Simakova, A.; Matyjaszewski, K.; *Polymer* **2015**, *60*, 302.
- Wu, W.; Wang, W.; Li, J.; *Prog. Polym. Sci.* **2015**, *46*, 55.
- Matyjaszewski, K.; Davis, T.; *Handbook of Radical Polymerization*, Wiley-Interscience: Hoboken, NJ, 2002.

14. Sawamoto, M.; Kamigaito, M.; *Chemtech* **1999**, 29, 30.
15. Matyjaszewski, K.; *Chem. Eur. J.* **1999**, 5, 3095.
16. Matyjaszewski, K.; Xia, J.; *Chem. Rev.* **2001**, 101, 2921.
17. Kamigaito, M.; Ando, T.; Sawamoto, M.; *Chem. Rev.* **2001**, 101, 3689.
18. Simal, F.; Demonceau, A.; Noels, A. F.; *Angew. Chem. Int. Ed.* **1999**, 38, 538.
19. Bielawski, C. W.; Louie, J.; Grubbs, R. H.; *J. Am. Chem. Soc.* **2000**, 122, 12873.
20. Charvet, R.; Novak, B. M.; *Macromolecules* **2004**, 37, 8808.
21. Cheng, C.; Khoshdel, E.; Wooley, K. L.; *Nano Lett.* **2006**, 6, 1741.
22. Simal, F.; Delfosse, S.; Demonceau, A.; Noels, A. F.; Denk, K.; Kohl, F. J.; Weskamp, T.; Herrmann, W. A.; *Chem. Eur. J.* **2002**, 8, 3047.
23. Lee, J.; Grandner, J. M.; Engle, K. M.; Houk, K. N.; Grubbs, R. H.; *J. Am. Chem. Soc.* **2016**, 138, 7171.
24. Dragutan, V.; Dragutan, I.; *J. Organomet. Chem.* **2006**, 691, 5129.
25. Lugo, C. A.; Lagadec, R. L.; Ryabov, A. D.; Valverde, G. C.; Morales, L. S.; Alexandrova, L.; *J. Polym. Sci., Part A: Polym. Chem.* **2009**, 47, 3814.
26. Clercq, B. D.; Verpoort, F.; *J. Mol. Catal. A - Chem.* **2002**, 180, 67.
27. Alfredo, N. V.; Lugo, C. A.; Gonzalez, O. D.; Lagadec, R. L.; Alexandrova, L.; *Macromol. Symp.* **2013**, 325-326, 10.
28. Diaz, M. O. G.; Morales, S. L.; Lagadec, R. L.; Alexandrova, L.; *J. Polym. Sci. Part A: Polym. Chem.* **2011**, 49, 4562.
29. Ando, T.; Kamigaito, M.; Sawamoto, M.; *Macromolecules* **2000**, 33, 6732.

Submitted: August 5, 2016

Published online: December 6, 2016